

Research article

Synthesis and Characterization of MgFe₂O₄(0.5)/TiO₂(0.5) Nano Ceramic pigment by mechano- chemical synthesis

T.Dayakar, K.Venkateswara Rao, Ch.Shilpa Chakra,

Centre for Nano Science and Technology, Institute of Science and Technology,
Jawaharlal Nehru Technological University Hyderabad, India.
JNTUH, Hyderabad
Phone no: +91-9440858664

E-mail: kalagadda2003@gmail.com

ABSTRACT

MgFe₂O₄ nanoparticles were synthesized by a solution combustion technique, taking precursor nitrate and fuel in appropriate ratio and TiO₂ nanoparticles are prepared by wet grinding technique and the composition of MgFe₂O₄/TiO₂ nanoceramic prepared by mechano chemical synthesis and are taken in equal wt%, x=0.5. The process was a simple, convenient, environment friendly, inexpensive and efficient method for synthesis of MgFe₂O₄/TiO₂ nanoceramic than the other preparation methods, controls particle size properties of materials. The synthesized nanoparticles were characterized by XRD, TGA, FTIR, UV-Visible, PSD, SEM, the material exhibits more optical and thermal properties which was suitable for the pigmentation property and also as environment friendly nano paint. **Copyright © IJNST, all rights reserved.**

Keyword: Nanostructure MgFe₂O₄, Anatase TiO₂, Optical and Thermal properties, SEM.

INTRODUCTION

In recent years, a considerable amount of interest in ceramic pigments has been focused on the photodegradation of organic pollutants through nano scale semiconductor powders [1]. Among semiconductor photocatalysts, TiO₂ has been extensively used due to its outstanding photocatalytic activity. However, there are two main disadvantages in the application of TiO₂. One limitation is the rapid recombination of photogenerated electron-hole pairs. The other disadvantage is the limitation of utilizing visible light because TiO₂ is only sensitive to UV light due to its large bandgap (3.2 eV for the anatase phase and 3.0 eV for the rutile phase). Therefore, numerous methods were proposed to enhance the photocatalytic activity of TiO₂ such as the incorporation of metal cations or non-metal anions into the TiO₂ matrix, the introduction of oxygen vacancies into the TiO₂ lattices, and the combination of two different semiconductors [2-4]. Among all the effective methods for the separation of photo induced electron-hole pairs, attention is increasingly focused on semiconductor combination. The main feature of this method is the formation of a composite semiconductor material. The formation of a coupled structure between a narrow-bandgap semiconductor and TiO₂ with matching band potentials provides an effective way to extend the photosensitivity of TiO₂ into the visible region. When excited by visible light, the electrons or holes photogenerated from the narrow-bandgap semiconductor can be transferred to TiO₂, initiating a photocatalytic

reaction [5–8]. Therefore, the combined photocatalysts usually exhibit excellent photocatalytic activity, attracting considerable attention. At present, a large variety of coupling photocatalysts have been reported such as $\text{ZnFe}_2\text{O}_4/\text{TiO}_2$ [9], $\text{MnFe}_2\text{O}_4/\text{TiO}_2$ [10], $\text{NiFe}_2\text{O}_4/\text{TiO}_2$ [11], $\text{CuFe}_2\text{O}_4/\text{TiO}_2$ [12], and so on. Magnesium ferrite (MFO) is a semiconductor with a spinel structure. MFO can absorb visible light due to its small bandgap (2.0 eV) and is not sensitive to photoanodic corrosion [13]. Hence, this material is considered a potential solar energy material for photoelectric conversion. MFO is also extensively investigated as a catalyst for the hydroxylation of phenol [14]. Kim et al. reported recently that MFO demonstrates capability in the photocatalytic degradation of 2-propanol [15]. Their findings indicate that MFO can also be a pigment property. MFO is believed to possess the potential to be developed into an efficient pigment for air or water purification due to its desirable properties in terms of photoabsorption and photocorrosion resistance. However, to the best of the authors' knowledge, no result corresponding to that from the study of Kim et al. had been reported. In the present study, MFO/ TiO_2 coupling pigment was synthesized using a mechano chemical synthesis. The physicochemical behavior of this material and its application as inorganic ceramic pigment was evaluated.

MATERIALS AND METHODS

Powder preparation

In this study MgFe_2O_4 nanoparticles were prepared using solution combustion technique. The materials used as precursors were magnesium nitrate hexahydrate $\text{Mg}(\text{NO}_3)_2 \cdot 6\text{H}_2\text{O}$, Iron nitrate hexahydrate $\text{Fe}(\text{NO}_3)_3 \cdot 6\text{H}_2\text{O}$ and glycine (all these were purchased from AR Grade of Qualigenfine Ltd. India). All of them were of high purity (99.9%, 98%, and 99.9% respectively). Glycine possesses a high heat of combustion. It is an organic fuel providing a platform for redox reactions during the course of combustion. Initially the magnesium nitrate, iron nitrate and are taken in the ratio 1:2 respectively and glycine were dissolved in a beaker slowly stirring by using magnetic stirrer clear solution was obtained. Then they formed solution was evaporated on hot plate in the temperature range of 70°C to 80°C resulting into a thick gel. The gel was kept on a hot plate for auto combustion and heated in the temperature range of 170°C to 180°C . The MgFe_2O_4 nanoparticles were formed within a few minutes and it was sintered at about 300°C , for about 2h, we then got a brown colour nanoparticles of MgFe_2O_4 [8-9] and bulk anatase TiO_2 structure were wet grinding for 1 hr to make nano size particles, then the composition of $\text{MgFe}_2\text{O}_4/\text{TiO}_2$ nanoparticles prepared by in equal 0.5wt%, then the samples are grounded in a mortar with pastel for 2 hr and calcinated for the temp at 500°C hence the prepared method was mechano-chemical synthesis,

RESULT AND DISCUSSION

The prepared samples were characterized by XRD Philips Analytic X-ray B.V. (PW-3710 Based model diffraction analysis using $\text{Cu-K}\alpha$ radiation), TG/DTA thermal analyzer (SDT Q600 V 20.9 Build 20), FTIR (Model no: Perkin Elmer precisely FT-IR spectrometer), Particle size analyzer (HORIBA SZ-100), SEM (HITACHI S3400N).

XRD analysis

This result shows that the structure of the $\text{MgFe}_2\text{O}_4/\text{TiO}_2$ composites was analyzed using XRD. Fig.1 shows the XRD patterns of $\text{MgFe}_2\text{O}_4/\text{TiO}_2$ with equal wt% calcinations at 773 K for 2 h. The pure TiO_2 is in the anatase phase (JCPDS 00-021-1272), whereas the pure MgFe_2O_4 is in the spinel phase (JCPDS 01-036-0398). The diffraction peaks of the MgFe_2O_4 are sharp and intense, revealing the highly crystalline character of the sample. The diffraction peaks of TiO_2 are broad and weak, indicating a small crystal size were 27.25, 25.36, 18.84. When the amount of doped $\text{MgFe}_2\text{O}_4(1-x)/\text{TiO}_2(x)$ where $x=0.5$. The diffraction peaks area of MgFe_2O_4 and TiO_2 peak area are equal, indicating that TiO_2 may be highly dispersed in the sample and no new phase was detected, indicating that the calcination of $\text{MgFe}_2\text{O}_4/\text{TiO}_2$ would not generate a new phase. The extended peaks observed and the corresponding to the (h k l) values shown in Fig.1 respectively. The lattice parameters were in good agreement with JCPDS card number of $\text{MgFe}_2\text{O}_4(1-x)/\text{TiO}_2(x)$.

The crystallite size is calculated by Debye – Scherrer’s formula,

$$D = \frac{K\lambda}{\beta \cos(\theta)}$$

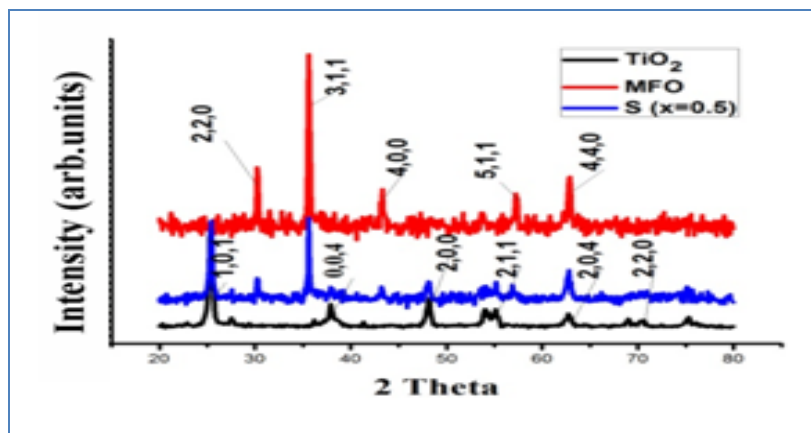


Figure.1: XRD pattern of $MgFe_2O_4$, TiO_2 and sample $(MgFe_2O_{4(1-x)}/TiO_{2(x)})$ where $x=0.5$ wt%

TG/DTA analysis

The TG/DTA curve in Fig.2.a shows When the temperature was increased from room temperature to $800^{\circ}C$ a minor weight loss, was observed so this prepared material is more pure form and high thermal stability, $MgFe_2O_4$, TiO_2 and $S(x=0.5)$ having 1.95, 4.45, 1.63 wt% loss. The minor weight loss was related to the loss of moisture and trapped solvent (water and carbon dioxide) in the $MgFe_2O_4$ nanopowder, whereas the major weight loss was due to the combustion of organic matrix. On the DTA curve, main exothermic peaks were observed at $290^{\circ}C$ and $400^{\circ}C$, suggesting the thermal events related to the decomposition of Mg and Fe nitrates along with the degradation by dehydration on the nanopowder, which was confirmed by a dramatic weight loss in TG curve at the corresponding temperature. The plateau formed between $350^{\circ}C$ and $800^{\circ}C$ on the TG curve indicated the formation of $MgFe_2O_4$, TiO_2 as the decomposition product, As confirmed by XRD and FT-IR analyses.

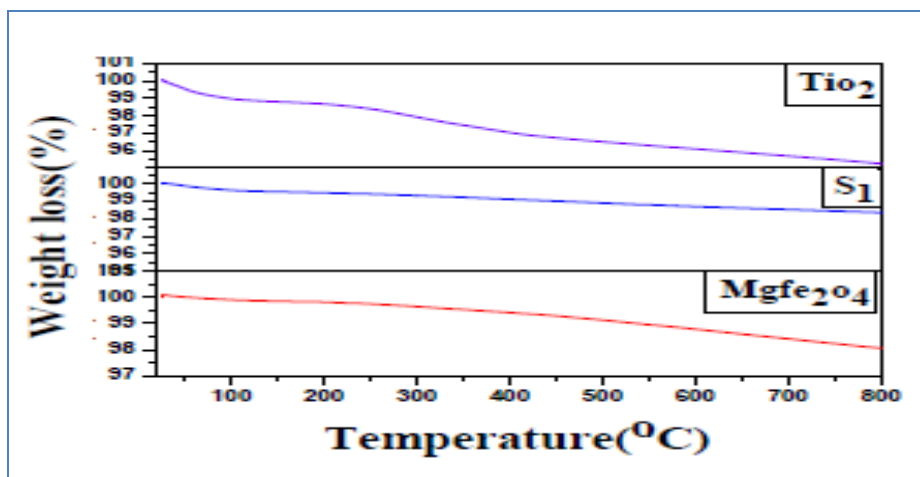


Figure 2.a: TG/DTA curves of $MgFe_2O_4$, TiO_2 and sample $(MgFe_2O_{4(1-x)}/TiO_{2(x)})$ where $x=0.5$ wt%

Fig.2.b shows the rate of heat flow at particular temperature represents the thermal conductivity of material, $MgFe_2O_4$, TiO_2 , has maximum broad exothermic peak centered at $150^\circ C$ for $MgFe_2O_4$ and TiO_2 is $280^\circ C$ which was probably caused by the formation of Fe_2O_3 from $Fe(OH)_3$ [11]. Both the TG and DTA curves are rough below $380^\circ C$ indicated that the crystallites were formed in a wide temperature range, due to having spinal structure for $MgFe_2O_4$ and different from structure for TiO_2 However, the dried gel had a weight loss of about 87% in the same temperature range. The DTA curve exhibits a sharp exothermic peak at $224^\circ C$, and the TG curve shows that most of the weight loss also occurred around this temperature, it probably resulted from the oxidation of organic matter. It is noticeable that the TG curve becomes smooth and the DTA curve rises linearly with increasing temperature implying that almost all the crystallites were formed below $270^\circ C$ Comparing with the coprecipitation method, the sol-combustion method facilitated the formation of $MgFe_2O_4$ crystallites at lower temperature.

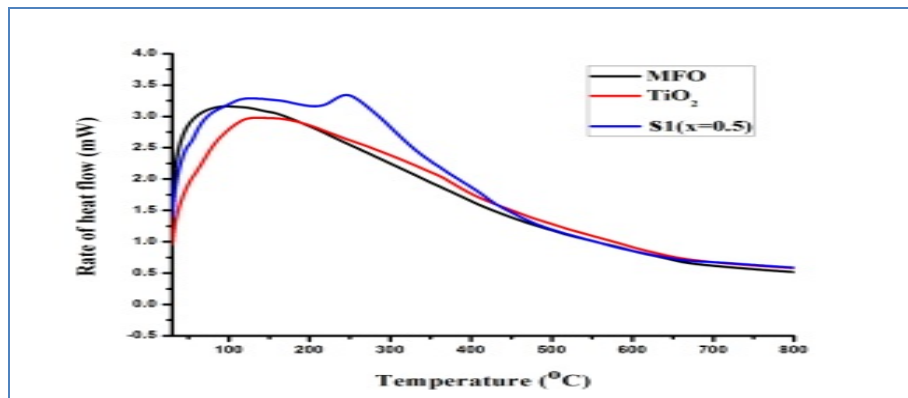


Figure 2.b: TG/DTA curve shows the rate of heat flow of the $MgFe_2O_4$, TiO_2 and sample (where $x=0.5wt\%$)

Uv-visible spectroscopy

Fig. 3.1.a shows the UV-vis absorption of MFO, TiO_2 , and MFO/ TiO_2 composites with $x=0.5$ concentration. The absorption edges of MFO/ TiO_2 shift to a longer wavelength compared with those of pure TiO_2 , and the absorption intensity is also enhanced indicates blue shift, as absorption wavelength decreases due to decreasing in particle size and increases the energy band gap due quantum confinement occurs in the prepared sample $x=0.5$ then the MFO, TiO_2 . Generally, the formation energy band gap increases is determined by the photo absorption capability. The increased absorption wavelength range enables an MFO/ TiO_2 catalyst to obtain a high level of photocatalytic activity and prepared sample is having high absorption, transmittance, reflectance properties, suitable for the pigment/for nano paint, the MFO, TiO_2 can shows different colors at different temperature.

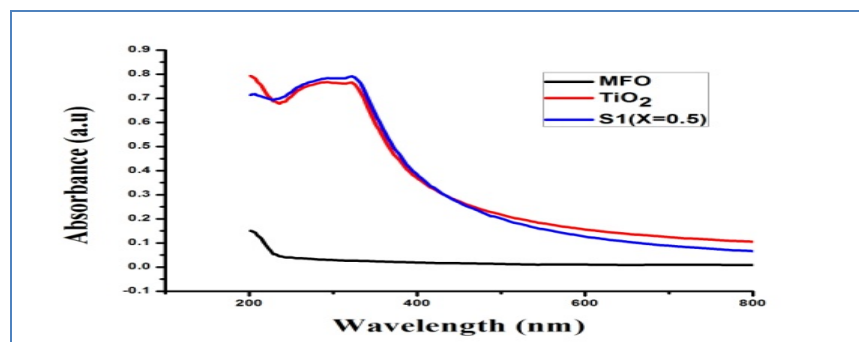


Figure 3.1.a: UV-vis absorption spectra of $MgFe_2O_4$, TiO_2 and sample (where $x=0.5wt\%$)

From fig 3.1.b shows the energy band gap of nano particles is compared with bulk materials. The energy band gap for bulk $MgFe_2O_4$ and TiO_2 nano materials is 2.12eV and 3.21eV. The fundamental absorption, which corresponds to electron excitation from the valence band to conduction band, can be used to determine the value of the optical band gap. The Tauc relation between the absorption coefficient (α) and the incident photon energy ($h\nu$) can be written as $(\alpha h\nu)^2 = A(h\nu - E_g)^n$

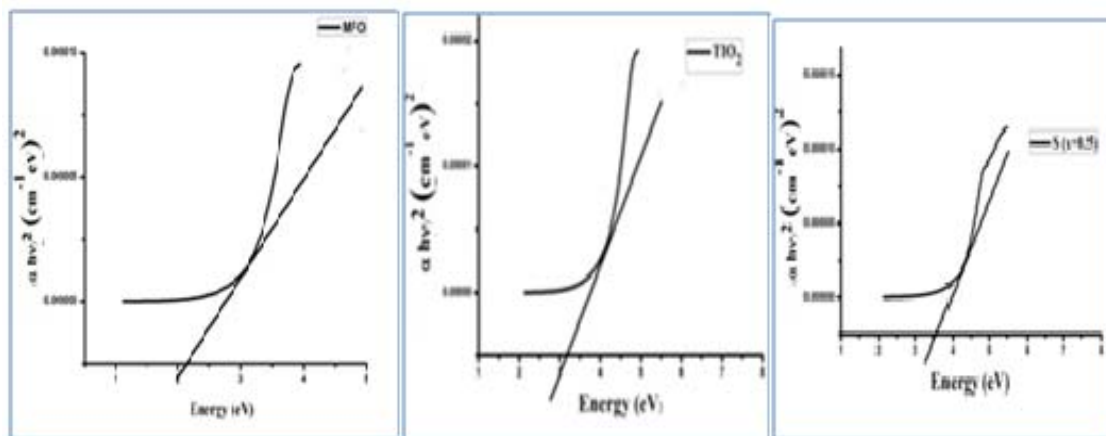


Figure 3.1.b: UV–vis spectra shows energy band gap drawn from Tauc relation of $MgFe_2O_4$, TiO_2 and sample (where $x=0.5wt\%$)

The energy band gap is measured with the help of absorption spectrum and a graph of $(\alpha h\nu)^2$ versus $h\nu$ is plotted in Fig.3.1.b. The extrapolation of the straight line to $(\alpha h\nu)^2 = 0$ gives the value of the energy band gap of prepared $MgFe_2O_4$ and TiO_2 nano particles. That is for sample s1 gives an increase in the band gap is observed was 3.52eV due to the quantum confinement effects in the nano particles with the change in a blue shift was observed which indicates the decrease in particle size are shown in table 1.

Particle size distribution studies

Particle size distribution has been carried out by using dynamic light scattering techniques. (DLS via Laser input energy of 632 nm) The as-prepared nanoparticles were ultra-sonicated and suspended in the ethanol solution.

Table 1: XRD and PSA nm range

	XRD CRYSTALLINE SIZE(nm)	PARTICLE SIZE ANALYSER (PSA) (nm)
$MgFe_2O_4$	27.25	32.5
TiO_2	25.36	28.5
X=0.5	18.84	22.5

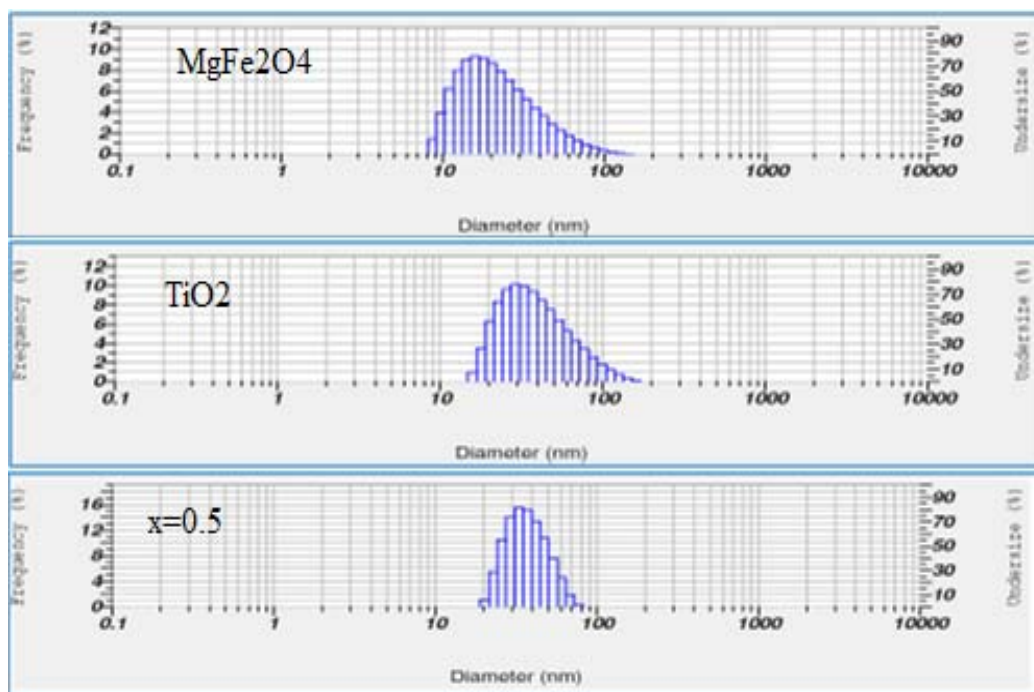


Figure 4: particle size distribution histograms of MgFe_2O_4 , TiO_2 and sample (where $x=0.5$ wt%)

The sizes of the agglomerated colloids in the suspensions were estimated using particle size analyzer. The histograms of the particle sizes versus under size percentages are shown below. It was observed that MgFe_2O_4 and TiO_2 nanoparticles have narrow size distribute which was mentioned in the table 1. Which are well match with calculated value from Debye-Scherrer equation obtained from XRD.

FT-IR analysis

Fourier Transform Infrared Spectroscopy (FTIR) is a non-destructive analytical technique used to identify mainly organic materials. FTIR analysis results in absorption spectra which provide information about the chemical bonds and molecular structure of a material for MgFe_2O_4 . In the range of $4000\text{--}1000\text{ cm}^{-1}$, vibrations of CO_3^{2-} and moisture were observed. The intensive band at 1627 cm^{-1} is due to O–H stretching vibration interacting through H bonds. The band at 3436 cm^{-1} is C–H asymmetric stretching vibration mode due to the CH_2^- groups of the long aliphatic alkyl groups. The $\nu(\text{C}=\text{O})$ stretching vibration of the carboxylate group (CO_2^{2-}) was observed around 1580 cm^{-1} . The band observed at 559 cm^{-1} is attributed to the tetrahedral group the band at 450 cm^{-1} is assigned to the octahedral group. FT-IR spectra for synthesized TiO_2 band at $3000\text{--}3500\text{ cm}^{-1}$ corresponding to stretching vibrations $\nu(\text{OH})$ of hydroxyl groups. Peaks at 1650 cm^{-1} is OH. The band at $400\text{--}500\text{ cm}^{-1}$ corresponding to the vibration of the Ti–O bonds in the TiO_2 . The shift in the lower no of the O–Ti–O band width increase may be assumed to be due to decrease in size of the nanoparticles. All the peaks was observed in the prepared sample

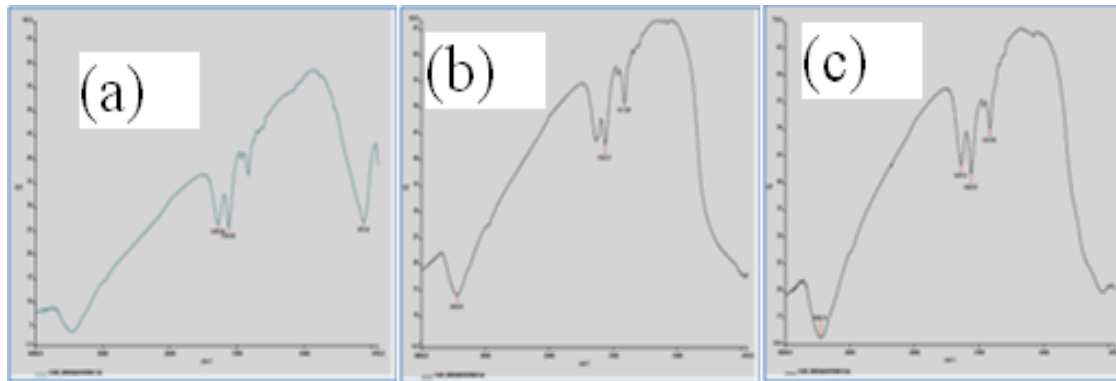


Figure 5: FTIR spectra of (a) MgFe_2O_2 (b) Anatase TiO_2 (c) Sample ($x = 0.5\text{wt} \%$)

SEM

Obtained image of Fig.6.a show remarkable change in the structure regarding porosity, grain size of sample. From fig it can be concluded that frothy and small holes within structure, which may be due to escaping large number of gases during the combustion. It can be seen from figure that sample exhibit network with voids and pores. The porosity in all cases is found to be entirely intergranular. The formation of pores is attributed to the release of large amount of gases during combustion process. From fig 6.b the formation of multigrain

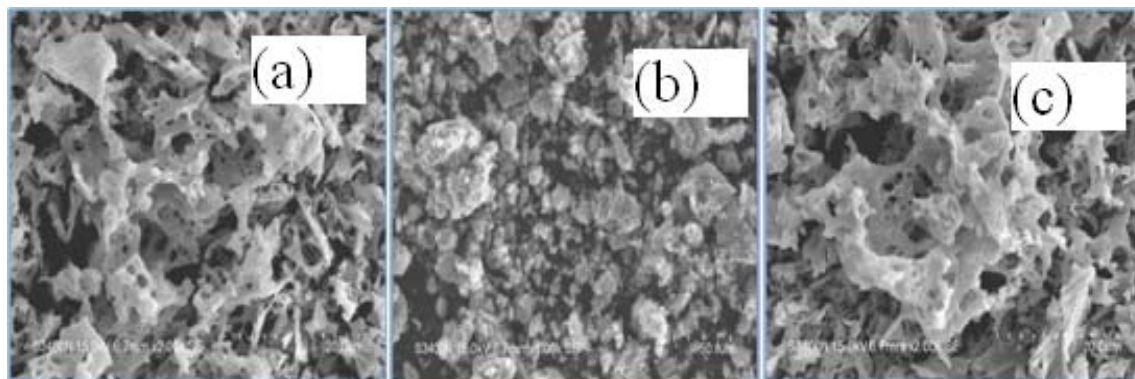


Figure 6: SEM images of (a) MgFe_2O_2 (b) Anatase TiO_2 (c) Sample ($x = 0.5\text{wt} \%$)

agglomerates observed in all samples consists of very fine crystallites as they show strong tendency to form agglomerates [12]. The appearance of spongy structure was attested a better crystallinity of spinel phase. From fig 6.c the equal amount of wt% used in this case results in a small enthalpy and hence the local temperature of the particles remains low, which may prevent the formation of adense structure. Associated gas evolution results in highly porous structure, i.e., as the amount of gas increases agglomerates are more likely to break up .

Conclusion

The observation started at mixing of wt 0.5 % of MgFe_2O_4 / TiO_2 , but especially at the 0.5wt % of TiO_2 it dominates the peaks of MgFe_2O_4 . Average crystallite size is 18.84 nm. Most of the particle distribution is in the range of 15-35nm. From UV-Vis Transmittance and as well as energy gap analysis we observed that Transmittance decreases and band gap increases in the samples wt 0.5 % of TiO_2 , TG-DTA implying that almost all the crystallites were formed below 470°C the formation of MgFe_2O_4 crystallites at lower temperature. From the TG-DTA analysis it shows that the samples have the thermal stability in high degree of precision. From the appearance of spongy structure was attested a better crystallinity of spinel phase. Associated gas

evolution results in highly porous structure, i.e., as the amount of gas increases agglomerates are more likely to break up, the material shows high thermal and optical properties make more efficient for pigment/nano paint.

Acknowledgement

One of the authors T.Dayakar, is thankful to Head of the CNST, IST, JNTUH and DST Nano mission for providing the facilities and funds.

References

- [1] Fujishima., T.N. Rao., and D.A. Tryk., "Titanium dioxide photocatalysis," J. Photochem Photobiol, C Photochem., Rev. 1 (2000), pp. 1–21.
- [2] A.L. Linsebigler., G. Lu., and J.T. Yates Jr., "Photocatalysis on TiO₂ surfaces: Principles, mechanisms, and selected results," hem. Rev., 95 (1995), pp. 735–758.
- [3] M.A. Fox., and M.T. Dulay., "Heterogeneous photocatalysis," Chem. Rev., 93 (1993), pp. 341–357.
- [4] C.C.Wong., and W.Chu., "The hydrogen peroxide-assisted photocatalytic degradation of alachlor in TiO₂ suspensions," Environ. Sci. Tech., 37 (2003), pp. 2310–2316.
- [5] F. Chen., Y.D. Xie., J.C. Zhao., and G.X. Lu., "Photocatalytic degradation of dyes on a magnetically separated photocatalyst under visible and UV irradiation," Chemosphere ., 44 (2001), pp. 1159–1168.
- [6] S. Rana., R.S. Srivastava., M.M. Sorensson., and R.D.K. Misra., "Synthesis and characterization of nanoparticles with magnetic core and photocatalytic shell: AnataseTiO₂–NiFe₂O₄ system," Mater.Sci. Eng., B 119 (2005), pp. 144–151.
- [7] H.B. Yang., W.Y. Fu., L.X. Chang., H. Bala., M.H. Li., and G.T. Zou., "Anatase TiO₂ nanolayer coating on strontium ferrite nanoparticles for magnetic photocatalyst," Colloid Surf. A Physicochem. Eng., Asp. 289 (2006), pp. 47–52.
- [8] R. Jain., M. Mathur., S. Sikarwar., A. Mittal., J. Environ. Manage., 85 (2007), 956– 964.
- [9] W. Choi., Catal., Surv. Asia 10., (2006), 16–28.
- [10] M.A. Shannon., P.W. Bohn., M. Elimelech., J.G. Georgiadis., B.J. Marinas., A.M. Mayes., Nature 452 (2008), 301–310.
- [11] A. Kezzim., N. Nasrallah., A. Abdi., M. Trari., Energy Convers. Manage., 52 (2011).
- [12] Khetre S.M., Jadhav H.V., Jagdale P.N., Bangale S.V., Bamane S.R., Advances in Applied Science Research , (2011) , 2, (2) , 252-259.
- [13] Bangale S. V., Khetre S. M. and Bamane S. R., Advances in Applied Science Research , (2011),2, 252-259.
- [14] Sachin V.Bangale., and Sambhaji R. Bamane., Archives of Applied Science Research Vol. 3 No. 4, (2011), 300-308.
- [15] Cullity B.D., Stock S.R., Elements of X-ray Diffraction., Prentice Hall, NJ, (2001).